Experimental investigation of vinyl chloride polymerization at high conversion: molecular-weight development

T. Y. Xie, A. E. Hamielec*, P. E. Wood and D. R. Woods
Institute for Polymer Production Technology, Department of Chemical Engineering, McMaster University, Hamilton, Ontario, Canada L8S 4L7
(Received 20 February 1990; accepted 29 April 1990)

A comprehensive model for molecular-weight development during the suspension polymerization of vinyl chloride has been developed. The poly(vinyl chloride) (PVC) was characterized by low-angle laser light scattering (LALLS) and gel permeation chromatography calibrated using the results of LALLS measurements. Kinetic parameters were estimated using accumulated molecular weights measured at different conversions and polymerization temperatures. The present model is in excellent agreement with the experimental accumulated number-, weight- and *Z*-average molecular weights and distribution data over the entire conversion range. The mechanisms of termination and chain transfer and the effect of conversion, monomer and initiator concentrations and polymerization temperature on molecular-weight development are discussed in some detail. The present model predicts instantaneous molecular weights and distributions in each phase, the total instantaneous and accumulated molecular-weight averages, and instantaneous and accumulated molecular-weight distributions as functions of the reactor operational conditions, and can satisfactorily explain the kinetic features of PVC molecular-weight development.

(Keywords: vinyl chloride; poly(vinyl chloride); molecular-weight average and distribution; two-phase polymerization; kinetic and suspension reactor modelling)

INTRODUCTION

Poly(vinyl chloride) (PVC) molecular-weight development has been extensively investigated experimentally for bulk, suspension, emulsion and solution polymerization processes over wide temperature ranges. The main findings were as follows.

The molecular weight of PVC does not depend strongly on process type, monomer conversion[1–7] and initiator concentration[3–5] for isothermal polymerization, but it increases significantly with decreasing polymerization temperature[5,7–9]. These phenomena are attributed to the dominance of chain transfer to monomer in controlling PVC molecular-weight development.

At high conversions (under subsaturation pressure), the number-average molecular weight decreases with conversion significantly while the weight-average molecular weight decreases only slightly, so that the molecular-weight distribution (*MWD*) becomes broader and the polydispersity increases with decreasing reactor pressure[4,10–14].

Molecular-weight modelling has, however, not been studied extensively and a few attempts have had limited success under subsaturation conditions because of a lack of molecular-weight data measured over a wide range of polymerization conditions. Abdel-Alim *et al.*[5] first developed a model for accumulated molecular-weight average and distribution for PVC assuming homogeneous kinetics to be valid to both monomer and polymer phases. The model does not predict the fall in accumulated number-average molecular weight and the increasing polydispersity at high conversions that has been shown experimentally[4,10–14]. Kelsall *et al.*[15], more recently, proposed a model for the calculation of molecular-weight average for PVC. The model predicts that the accumulated number-average molecular weight increases with conversion significantly. It is clearly in contradiction to the experimental results mentioned above.

As discussed in a previous publication[16], vinyl chloride (VCM) polymerization involves a larger number of elementary reactions than previously known. The objective of this investigation is to develop a comprehensive model that can predict instantaneous and accumulated molecular-weight average and distribution for PVC made by bulk and suspension polymerization. The model should account for all of the relevant elementary reactions[16] and include the parameters estimated using comprehensive experimental data over wide ranges of synthesis conditions to ensure narrow confidence intervals for the kinetic parameters.

MODEL DEVELOPMENT

The basic assumptions made in the polymerization rate modelling[16] are again employed for molecular-weight modelling.

During free-radical polymerization, live and dead macromolecules have chain-length distributions. For any distribution function it is possible to define a series of moments. The *i*th moments for the dead and live polymer

* To whom correspondence should be addressed

0032-3861/91/061098-14
© 1991 Butterworth-Heinemann Ltd.

distribution Q_i and Y_i are defined as:

$$Q_i = \sum_{r=1}^{\infty} r^i P_r \tag{1}$$

$$Y_i = \sum_{r=1}^{\infty} r^i R_r^{\cdot} \tag{2}$$

where i is zero or a positive number (nomenclature is given at end of paper).

When conversion is less than X_f, the conversion at which the monomer phase is consumed, polymer is produced in both monomer and polymer phases simultaneously. Hence, the moment equations will be derived for both phases.

Molecular-weight development in the monomer phase

In the monomer phase, chain transfer to polymer can be neglected because of very low concentration of dead polymer. Bimolecular termination between polymer and primary radicals should be insignificant because of the very low concentration of primary radicals compared to that for polymer radicals, and is neglected. Therefore, the rate of polymer production in the monomer phase can be expressed as:

$$\frac{dP_r}{V_1\,dt} = K_{td1}[R^{\cdot}]_1[R_r^{\cdot}]_1 + \frac{K_{tc1}}{2}\sum_{s=1}^{r-1}[R_s^{\cdot}]_1[R_{r-s}^{\cdot}]_1 + K_{fm1}[M]_1[R_r^{\cdot}]_1 \qquad (2 \leqslant r < r_c) \tag{3}$$

$$\frac{dP_1}{V_1\,dt} = K_{td1}[R^{\cdot}]_1[R_1^{\cdot}]_1 \qquad (r = 1) \tag{4}$$

where the subscript 1 on the concentrations (square brackets) stands for monomer phase. Subscripts are not used on the total moles of polymer of chain lengths r and 1 in the monomer phase (P_r and P_1). Chain lengths equal to or greater than r_c for both live and dead polymer molecules do not exist in the monomer phase[16]. Chain transfer to monomer involves more than one elementary reaction. This has been discussed earlier[16].

Using the definition of the moments and summing equations (3) and (4) over all chain lengths, the following moment equations may be derived for the monomer phase:

$$\frac{dQ_{0m}}{V_1\,dt} = (K_{td1} + \tfrac{1}{2}K_{tc1})[R^{\cdot}]_1^2 + K_{fm1}[R^{\cdot}]_1[M]_1 \tag{5}$$

$$\frac{dQ_{1m}}{V_1\,dt} = K_{p1}[M]_1[R^{\cdot}]_1 \tag{6}$$

$$\frac{dQ_{2m}}{V_1\,dt} = \{(K_{td1} + K_{tc1})[R^{\cdot}]_1 + K_{fm1}[M]_1\}Y_{2m} + K_{tc1}Y_{1m}^2 \tag{7}$$

$$\frac{dQ_{3m}}{V_1\,dt} = \{(K_{td1} + K_{tdc1})[R^{\cdot}]_1 + K_{fm1}[M]_1\}Y_{3m} + 3K_{tc1}Y_{1m}Y_{2m} \tag{8}$$

where the subscript m on the moments stands for monomer phase.

The solution of equations (7) and (8) requires a knowledge of the moments of the polymer radical distribution. The polymer radical balances can be written as

$$\frac{dR_r^{\cdot}}{V_1\,dt} = K_{p1}[M]_1[R_{r-1}^{\cdot}]_1 - K_{p1}[M]_1[R_r^{\cdot}]_1 - (K_{td1} + K_{tc1})[R^{\cdot}]_1[R_r^{\cdot}]_1 - K_{fm1}[M]_1[R_r^{\cdot}]_1 + K_{de}[R_r^{\cdot}]_2V_2/V_1 \qquad (2 \leqslant r_c < r) \tag{9}$$

$$\frac{dR_1^{\cdot}}{V_1\,dt} = R_{I1} + K_{fm1}[R^{\cdot}]_1[M]_1 - K_{p1}[M]_1[R_1^{\cdot}]_1 - (K_{td1} + K_{tc1})[R^{\cdot}]_1[R_1^{\cdot}]_1 + K_{de}[R_1^{\cdot}]_2V_2/V_1 \qquad (r = 1) \tag{10}$$

The desorption constant depends strongly on diameter of the primary particles, so that desorption of radicals from the polymer phase is significant only at very low conversions[16]. However, the reaction volume in the monomer phase is much larger than that in the polymer phase at very low conversions; hence, the effect of the desorption on the concentration of radicals with chain lengths r and 1 can be neglected. Therefore, the associated moment equations follow:

$$\frac{dY_{1m}}{V_1\,dt} = K_{p1}[M]_1[R^{\cdot}]_1 - (K_{td1} + K_{tc1})[R^{\cdot}]_1Y_{1m} - K_{fm1}[M]_1Y_{1m} + K_{fm1}[M]_1[R^{\cdot}]_1 + R_{I1} \tag{11}$$

$$\frac{dY_{2m}}{V_1\,dt} = K_{p1}[M]_1([R^{\cdot}]_1 + 2Y_1) - (K_{td1} + K_{tc1})[R^{\cdot}]_1Y_{2m} - K_{fm1}[M]_1Y_{2m} + K_{fm1}[R^{\cdot}]_1[M]_1 + R_{I1} \tag{12}$$

$$\frac{dY_{3m}}{V_1\,dt} = K_{p1}[M]_1([R^{\cdot}]_1 + 3Y_{1m} + 3Y_{3m}) - (K_{td1} + K_{tc1})[R^{\cdot}]_1Y_{3m} - K_{fm1}[M]_1Y_{3m} + K_{fm1}[M]_1[R^{\cdot}]_1 + R_{I1} \tag{13}$$

Applying the steady-state hypothesis to equations (11)–(13), one can express the first to third moments of the polymer radical distribution as:

$$Y_{1m} = \frac{K_{p1}[M]_1[R^{\cdot}]_1 + K_{fm1}[R^{\cdot}]_1[M]_1 + R_{I1}}{(K_{td1} + K_{tc1})[R^{\cdot}]_1 + K_{fm1}[M]_1} \tag{14}$$

$$Y_{2m} = \frac{K_{p1}[M]_1([R\cdot]_1 + 2Y_{1m}) + K_{fm1}[R\cdot]_1[M]_1 + R_{I1}}{(K_{td1} + K_{tc1})[R\cdot]_1 + K_{fm1}[M]_1} \tag{15}$$

$$Y_{3m} = \frac{K_{p1}[M]_1([R^{\cdot}]_1 + 3Y_{1m} + 3Y_{2m}) + K_{fm1}[R^{\cdot}]_1[M]_1 + R_{I1}}{(K_{td1} + K_{tc1})[R^{\cdot}]_1 + K_{fm1}[M]_1} \tag{16}$$

Substituting equations (14)–(16) for polymer radical moments in equations (7) and (8) one obtains:

$$\frac{dQ_{2m}}{V_1\,dt} = R_{p1}\left[\frac{(2 + \tau_1 + \beta_1)R_{cm}}{\tau_1 + \beta_1} + \beta_1\left(\frac{R_{cm}}{\tau_1 + \beta_1}\right)^2\right] \tag{17}$$

$$\frac{dQ_{3m}}{V_1\,dt} = R_{p1}\left(\frac{6\beta_1R_{cm}^2}{(\tau_1 + \beta_1)^3} + \frac{3R_{cm}(2 + \beta_1R_{cm})}{(\tau_1 + \beta_1)^2} + \frac{6R_{cm}}{\tau_1 + \beta_1} + R_{cm}\right) \tag{18}$$

where

$$R_{p1} = K_{p1}[M]_1[R^\cdot]_1 \qquad R_{cm} = 1 + CM_1 + R_{I1}/R_{p1}$$

$$\tau_1 = \frac{K_{td1}[R^\cdot]_1}{K_{p1}[M]_1} + CM_1 \qquad \beta_1 = \frac{K_{p1}[R^\cdot]_1}{K_{p1}[M]_1}$$

$$CM_1 = K_{fm1}/K_{p1}$$

The rate constant for chain transfer to monomer K_{fm1} has been derived in a previous publication[16] and is given by:

$$K_{fm1} = \frac{K_1 K_2 K_5}{(K_2 + K_3[M]_1)(K_4[M]_1 + K_5)} \tag{19}$$

With the moment equations (equations (5), (6), (17) and (18)) above, one can easily derive relationships for the instantaneous number-, weight- and Z-average molecular weights as follows:

$$(M_n)_m = \frac{M_m}{\tau_1 + (\beta_1/2)} \tag{20}$$

$$(M_w)_m = M_m\left[\frac{2R_{cm}}{\tau_1 + \beta_1} + \beta_1\left(\frac{R_{cm}}{\tau_1 + \beta_1}\right)^2\right] \tag{21}$$

$$(M_z)_m = M_m \frac{S_1^3 + 6(S_1^2 + S_1 + \beta_1 R_{cm}) + 3\beta_1 S_1 R_{cm}}{S_1(S_1^2 + 2S_1 + \beta_1 R_{cm})} \tag{22}$$

where

$$S_1 = \tau_1 + \beta_1$$

The instantaneous molecular-weight distribution (MWD) is defined as:

$$W(r)_m = \frac{r}{R_{p1}}\left(\frac{dP_r}{V_1\,dt}\right) \tag{23}$$

and can be calculated as follows. Applying the steady-state hypothesis to equations (9) and (10), one can find the concentration of polymer radical with chain length r as:

$$[R_r^\cdot]_1 = \left(\frac{1}{1 + \tau_1 + \beta_1}\right)^r\left(\frac{R_{I1}}{R_{p1}} + CM_1\right)[R^\cdot]_1 \tag{24}$$

Substituting equation (24) into equation (3), one has:

$$\frac{dP_r}{V_1\,dt} = R_{p1}\left[\tau_1\left(\frac{R_{I1}}{R_{p1}} + CM_1\right) + \frac{\beta_1}{2}(r-1)\left(\frac{R_{I1}}{R_{p1}} + CM_1\right)^2\right] \times \left(\frac{1}{1 + \tau_1 + \beta_1}\right)^r \tag{25}$$

Substituting equation (25) into equation (23), one obtains:

$$W(r)_m = r\left[\tau_1\left(\frac{R_{I1}}{R_{p1}} + CM_1\right) + \frac{\beta_1}{2}(r-1)\left(\frac{R_{I1}}{R_{p1}} + CM_1\right)^2\right] \times \left(\frac{1}{1 + \tau_1 + \beta_1}\right)^r \tag{26}$$

Equations (20)–(22) and (26) allow one to calculate the instantaneous molecular-weight averages and chain-length distribution in the monomer phase.

Molecular-weight development in the polymer phase

In the polymer phase, the concentration of polymer is high, about 70 wt% even at very low conversions. Therefore, polymer and chlorine radicals may transfer to dead polymer at a significant level and affect the molecular-weight development. However, the effect of primary radical termination and reaction with internal double bonds on molecular weight may be negligible due to the very low concentrations of these species, and they are neglected. A terminal double bond on the polymer chain is mainly formed by chain transfer to monomer (formation of 1-chloro-2-alkene structure as a result of abstraction of a chlorine radical[16]). However, the number of 1-chloro-2-alkene ($\sim CH_2-CH{=}CH-CH_2Cl$) and 1,2-dichloro-alkane ($\sim CH_2-CHCl-CH_2Cl$) structures for commercial PVC is almost the same[17]. This implies that the terminal double bond ($\sim CH_2-CH{=}CH-CH_2Cl$) is not active during VCM polymerization. On the other hand, the reaction with a terminal double bond should lead to the increase of number-average molecular weight with conversion, but the experimental results show that the number-average molecular weight hardly changes with conversion for $X < X_f$. Therefore, the reaction with a terminal double bond is neglected. Short-chain branches formed by back-biting reactions do not affect molecular-weight development and do not have to be accounted for in the molecular-weight calculations. Hence, the production rate of dead polymer with chain length r can be expressed as:

$$\frac{dP_r}{V_2\,dt} = K_{td2}[R^\cdot]_2[R_r^\cdot]_2 + \tfrac{1}{2}K_{tc2}\sum_{s=1}^{r-1}[R_s^\cdot]_2[R_{r-s}^\cdot]_2 + K_{fm2}[R_r^\cdot]_2[M]_2 + K_{fp}[R_r^\cdot]_2 Q_{1p}/V_2 - K'_{fp}[Cl^\cdot]_2 r[P_r]_2 - K_{fp}[R^\cdot]_2 r[P_r]_2 \qquad (r \geqslant 2) \tag{27}$$

$$\frac{dP_1}{V_2\,dt} = K_{td2}[R^\cdot]_2[R_1^\cdot]_2 + K_{fp}[R_1^\cdot]_2 Q_{1p}/V_2 + K'_{fp}[Cl^\cdot]_2[P_1]_2 - K_{fp}[R^\cdot]_2[P_1]_2 \qquad (r = 1) \tag{28}$$

Using equations (27) and (28), the moment equations may be derived as:

$$\frac{dQ_{0p}}{V_2\,dt} = R_{p1}\{\tau_2 + \tfrac{1}{2}\beta_2 - C'_p CM_2 Q_{1p}/(V_2[M]_2)\} \tag{29}$$

$$\frac{dQ_{1p}}{V_2\,dt} = K_{p2}[M]_2[R^\cdot]_2 \tag{30}$$

$$\frac{dQ_{2p}}{V_2\,dt} = \{(K_{td2} + K_{tc2})[R^\cdot]_2 + K_{fm2}[M]_2 + K_{fp}Q_{1p}/V_2\} \times Y_{2p} + K_{tc2}Y_{1p}^2 - (K'_{fp}[Cl^\cdot]_2 + K_{fp}[R^\cdot]_2)Q_{3p}/V_2 \tag{31}$$

$$\frac{dQ_{3p}}{V_2\,dt} = \{(K_{td2} + K_{tc2})[R^\cdot]_2 + K_{fm2}[M]_2 + K_{fp}Q_{1p}/V_2\}Y_{3p} + 3K_{tc2}Y_{1p}Y_{2p} - (K'_{fp}[Cl^\cdot]_2 + K_{fp}[R^\cdot]_2)Q_{4p}/V_2 \tag{32}$$

where

$$\tau_2 = \frac{K_{td2}[R^\cdot]_2}{K_{p2}[M]_2} + CM_2 \qquad \beta_2 = \frac{K_{tc2}[R^\cdot]_2}{K_{p2}[M]_2}$$

$$CM_2 = K_{fm2}/K_{p2} \qquad C'_p = K'_{fp}/K'_p$$

The rate constant of chain transfer to monomer can be expressed based on the mechanism discussed in a

previous publication[16] as:

$$K_{fm2} = \frac{K_1 K_2 K_5}{(K_2 + K_3[M]_2)(K_4[M]_2 + K_5)} \quad (33)$$

where K_1, K_2, K_3, K_4 and K_5 are assumed to be the same in both phases at $X < X_f$.

Similarly, the polymer radical balance in the polymer phase can be written as:

$$\frac{dR_r^\cdot}{V_2\,dt} = K_{p2}[M]_2[R_{r-1}^\cdot]_2 + K'_{fp}[Cl^\cdot]_2 r[P_r]_2 + K_{fp}[R^\cdot]_2 r[P_r]_2 - K_{p2}[M]_2[R_r^\cdot]_2 - (K_{td2} + K_{tc2})[R^\cdot]_2[R_r^\cdot]_2 - K_{fm2}[R_r^\cdot]_2[M]_2 - K_{fp}[R_r^\cdot]_2 Q_{1p}/V_2 - K_{de}[R_r^\cdot]_2 \quad (r \geqslant 2) \quad (34)$$

$$\frac{dR_1^\cdot}{V_2\,dt} = R_{I2} + K_{fm2}[M]_2[R^\cdot]_2 + K'_{fp}[Cl^\cdot]_2[P_1]_2 + K_{fp}[R^\cdot]_2[P_1]_2 - K_{p2}[M]_2[R_1^\cdot]_2 - (K_{td2} + K_{tc2})[R^\cdot]_2[R_1^\cdot]_2 - K_{fp}[R_1^\cdot]_2 Q_{1p}/V_2 - K_{de}[R_1^\cdot]_2 \quad (r = 1) \quad (35)$$

where the effect of precipitation of radicals from the monomer phase is neglected due to very low precipitation constant estimated in a previous publication[16]. The desorption of radicals from the polymer phase is also negligible at relatively high conversions as mentioned earlier. Hence, the moment equations can be derived from equations (34) and (35) as:

$$\frac{dY_{1p}}{V_2\,dt} = R_{I2} + K_{p2}[M]_2[R^\cdot]_2 + K_{fm2}[M]_2[R^\cdot]_2 + (K'_{fp}[Cl^\cdot]_2 + K_{fp}[R^\cdot]_2)Q_{2p}/V_2 - \{(K_{td2} + K_{tc2})[R^\cdot]_2 + K_{fm2}[M]_2 + K_{fp}Q_{1p}/V_2\}Y_{1p} \quad (36)$$

$$\frac{dY_{2p}}{V_2\,dt} = R_{I2} + K_{p2}[M]_2([R^\cdot]_2 + 2Y_{1p}) + (K'_{fp}[Cl^\cdot]_2 + K_{fp}[R^\cdot]_2)Q_{3p}/V_2 + K_{fm2}[M]_2[R^\cdot]_2 - \{(K_{td2} + K_{tc2})[R^\cdot]_2 + K_{fm2}[M]_2 + K_{fp}Q_{1p}/V_2\}Y_{2p} \quad (37)$$

$$\frac{dY_{3p}}{V_2\,dt} = R_{I2} + K_{p2}[M]_2\{[R^\cdot]_2 + 3(Y_{1p} + Y_{2p})\} + K_{fm2}[M]_2[R^\cdot]_2 + (K'_{fp}[Cl^\cdot]_2 + K_{fp}[R^\cdot]_2) \times Q_{4p}/V_2 - \{(K_{td2} + K_{tc2})[R^\cdot]_2 + K_{fm2}[M]_2 + K_{fp}Q_{1p}/V_2\}Y_{3p} \quad (38)$$

The concentration of chlorine radical is given as[16]:

$$[Cl^\cdot]_2 = K_{fm2}[R^\cdot]_2/K'_p$$

Applying the steady-state hypothesis to equations (36)–(38), one gets the moments of polymer radical distribution:

$$Y_{1p} = \frac{R_{I2} + K_{p2}[M]_2[R^\cdot]_2 + K_{fm2}[M]_2[R^\cdot]_2 + K_{cp}Q_{2p}/V_2}{(K_{td2} + K_{tc2})[R^\cdot]_2 + K_{fm2}[M]_2 + K_{fp}Q_{1p}/V_2} \quad (39)$$

$$Y_{2p} = \frac{R_{I2} + K_{p2}[M]_2([R^\cdot]_2 + 2Y_{1p}) + K_{fm2}[M]_2[R^\cdot]_2 + K_{cp}Q_{3p}/V_2}{(K_{td2} + K_{tc2})[R^\cdot]_2 + K_{fm2}[M]_2 + K_{fp}Q_{1p}/V_2} \quad (40)$$

$$Y_{3p} = \frac{R_{I2} + K_{p2}[M]_2\{[R^\cdot]_2 + 3(Y_{1p} + Y_{2p})\} + K_{fm2}[M]_2[R^\cdot]_2 + K_{cp}Q_{4p}/V_2}{(K_{td2} + K_{tc2})[R^\cdot]_2 + K_{fm2}[M]_2 + K_{fp}Q_{1p}/V_2} \quad (41)$$

where

$$K_{cp} = K'_{fp}[Cl^\cdot]_2 + K_{fp}[R^\cdot]_2$$

Substituting equations (39)–(41) into equations (31) and (32), one can rewrite the moment equations for the second and third moments as:

$$\frac{dQ_{2p}}{V_2\,dt} = R_{p2}\left[R_{cp} + 2\frac{R_{cp} + PQ_2}{S_2} + \beta_2\left(\frac{R_{cp} + PQ_2}{S_2}\right)^2\right] \quad (42)$$

$$\frac{dQ_{3p}}{V_2\,dt} = R_{p2}\left(\frac{6\beta_2(R_{cp} + PQ_2)^2}{S_2^3} + \frac{(R_{cp} + PQ_2)[6 + 3\beta_2(R_{cp} + PQ_3)]}{S_2^2} + \frac{3(2R_{cp} + PQ_2 + PQ_3)}{S_2} + R_{cp}\right) \quad (43)$$

where

$$R_{p2} = K_{p2}[M]_2[R\cdot]_2 \qquad R_{cp} = 1 + R_{I2}/R_{p2} + CM_2$$
$$PQ_2 = (C'_pCM_2 + C_p)Q_{2p}/(V_2[M]_2)$$
$$PQ_3 = (C'_pCM_2 + C_p)Q_{3p}/(V_2[M]_2)$$
$$S_2 = \tau_2 + \beta_2 + C_pQ_{1p}/(V_2[M]_2) \qquad C_p = K_{fp}/K_{p2}$$

With equations (29), (30), (42) and (43), one can derive relationships for the instantaneous number-, weight- and Z-average molecular weights in the polymer phase as follows:

$$(M_n)_p = \frac{M_m}{\tau_2 + \frac{1}{2}\beta_2 - C'_pCM_2Q_{1p}/(V_2[M]_2)} \quad (44)$$

$$(M_w)_p = M_m\left[R_{cp} + 2\frac{R_{cp} + PQ_2}{S_2} + \beta_2\left(\frac{R_{cp} + PQ_2}{S_2}\right)^2\right] \quad (45)$$

$$(M_z)_p = M_m\left(\frac{6\beta_2RQ_2^2}{S_2^3} + \frac{RQ_2(6 + 3\beta_2RQ_3)}{S_2^2} + \frac{3(RQ_2 + RQ_3)}{S_2} + R_{cp}\right) \times \left[R_{cp} + \frac{2RQ_2}{S_2} + \beta_2\left(\frac{RQ_2}{S_2}\right)^2\right]^{-1} \quad (46)$$

where

$$RQ_2 = R_{cp} + PQ_2 \qquad RQ_3 = R_{cp} + PQ_3$$

The instantaneous molecular-weight distribution in the polymer phase is similarly defined as:

$$W(r)_p = \frac{r}{R_{p2}}\left(\frac{dP_r}{V_2\,dt}\right) \quad (47)$$

Applying the steady-state hypothesis to equations (34)

and (35), one has:

$$[R_r^{\cdot}]_2 = \left(\frac{1}{1+S_2}\right)^r \left(\frac{R_{I2}}{K_{p2}[M]_2} + CM_2[R^{\cdot}]_2\right) + (C'_pCM_2 + C_p)\frac{[R^{\cdot}]_2}{[M]_2}\sum_{i=1}^{r}\frac{i[P_i]_2}{(1+S_2)^{r+1-i}} \quad (48)$$

Substituting equation (48) into equation (27), one obtains:

$$\frac{dP_r}{V_2\,dt} = R_{p2}\left\{\left[\left(\tau_2 + C_p\frac{Q_{1p}}{V_2[M]_2}\right)\left(\frac{R_{I2}}{R_{p2}} + CM_2\right) + \frac{1}{2}\beta_2(r-1)\left(\frac{R_{I2}}{R_{p2}} + CM_2\right)^2\right]\left(\frac{1}{1+S_2}\right)^r + \left(\tau_2 + C_p\frac{Q_{1p}}{V_2[M]_2}\right)C \times \sum_{i=1}^{r}\frac{i[P_i]_2}{(1+S_2)^{r+1-i}} - Cr[P_r]_2\right\} \quad (49)$$

where $C = (C'_pCM_2 + C_p)/[M]_2$.

Therefore, the instantaneous molecular-weight distribution in the polymer phase can be expressed as:

$$W(r)_p = r\left\{\left[\left(\tau_2 + C_p\frac{Q_{1p}}{V_2[M]_2}\right)\left(\frac{R_{I2}}{R_{p2}} + CM_2\right) + \frac{1}{2}\beta_2(r-1)\left(\frac{R_{I2}}{R_{p2}} + CM_2\right)^2\right]\left(\frac{1}{1+S_2}\right)^r + \left(\tau_2 + C_p\frac{Q_{1p}}{V_2[M]_2}\right)C \times \sum_{i=1}^{r}\frac{i[P_i]_2}{(1+S_2)^{r+1-i}} - Cr[P_r]_2\right\} \quad (50)$$

Equations (30), (42)–(46), (49) and (50) allow one to solve for instantaneous molecular-weight averages and chain length distribution in the polymer phase.

The total instantaneous molecular weight and distribution

The above equations permit one to calculate instantaneous molecular-weight average and *MWD* for each phase. The total instantaneous molecular-weight average and *MWD* depend on quantity of polymer produced in the different phases. The instantaneous mass fraction of polymer can be calculated using instantaneous polymerization rate in both phases, such as:

$$m_1 = \frac{R_{p1}V_1}{R_{p1}V_1 + R_{p2}V_2} \quad (51)$$

$$m_2 = 1.0 - m_1 \quad (52)$$

Therefore, the total instantaneous molecular weight and *MWD* can be expressed as a function of molecular weight and *MWD* in both phases, that is:

$$M_n = \frac{1}{m_1/(M_n)_m + m_2/(M_n)_p} \quad (53)$$

$$M_w = m_1(M_w)_m + m_2(M_w)_p \quad (54)$$

$$M_z = m_1\frac{(M_w)_m}{M_w}(M_z)_m + m_2\frac{(M_w)_p}{M_w}(M_z)_p \quad (55)$$

$$W(r) = m_1W(r)_m + m_2W(r)_p \quad (56)$$

At high conversions ($X > X_f$), polymerization proceeds in the polymer phase only. Therefore, the total instantaneous molecular-weight average and *MWD* are the same as those in the polymer phase. Thus, equations (53)–(56) are still valid for the conversion X more than X_f by setting $m_1 = 0$ and $m_2 = 1$.

Accumulated molecular-weight average and distribution

With the total instantaneous molecular-weight average and *MWD* given in equations (53)–(56), one can find the accumulated molecular-weight average and *MWD* by either integration or differentiation. However, for a two-phase polymerization system, the differentiation method seems more convenient as it avoids integration in two phases. Based on the definitions of molecular-weight average, the relationships between accumulated and instantaneous molecular-weight average and distribution are governed by the following differential equations (when long chain branching is negligible):

$$d(X/\bar{M}_n)/dt = R_p/M_n \quad (57)$$

$$d(X\bar{M}_w)/dt = R_pM_w \quad (58)$$

$$d(X\bar{\Psi}/dt = R_pM_wM_z \quad (59)$$

$$\bar{M}_z = \bar{\Psi}/\bar{M}_w \quad (60)$$

where

$$\bar{\Psi} = M_m^2\int_0^\infty r^2\bar{W}(r)\,dr \text{ and } \frac{d(X\bar{W}(r))}{dt} = R_pW(r) \quad (61)$$

where

$$R_p = dX/dt$$

The accumulated number-, weight- and *Z*-average molecular weights and chain-length distribution can be obtained by solving equations (57)–(61) using appropriate reactor operational conditions. These equations are valid over the entire conversion range.

EXPERIMENTAL

PVC was made by suspension polymerization. The detailed procedures for these polymerizations are given in a previous publication[16]. In this section, only details of the molecular-weight measurements will be described.

Molecular-weight measurements of PVC have been studied extensively by various methods[18–52]. Gel permeation chromatography (g.p.c.) is the most powerful analytical method providing the full molecular-weight distribution as well as molecular-weight averages. However, it is not an absolute method and must be calibrated. Universal calibration after Grubisic *et al.*[53] is used by most authors[5,6,29,31,40,41,47–51]. Many Mark–Houwink constants for PVC in g.p.c. solvent tetrahydrofuran (THF) and others have been published[20,21,24,26,31,32,40,42–46,52]. Unfortunately, the values for the Mark–Houwink constants vary widely. For PVC in THF, the values of Freeman *et al.*[20] and Bohdanecky *et al.*[26] have been widely used in the literature. Although the PVC samples were carefully fractionated in these studies[20,26], there was appreciable polydispersity, especially for higher molecular-weight fractions used. Because of these uncertainties, it was decided to calibrate the g.p.c. using PVC weight-average molecular weight measured by low-angle laser light scattering (LALLS).

LALLS measurements

A Chromatix KMX-6 low-angle laser light scattering (LALLS) photometer, with a cell length of 15 mm and a field stop of 0.2 corresponding to an average scattering angle of 4.8°, was used for $\bar{M}_w$ measurements. THF was used as a solvent. The concentration of PVC in the solution was in the range of $(0.5–5.0) \times 10^{-3}$ g ml^{-1}. The refractive index increment of PVC–THF solutions was determined using a Chromatix KMX-16 laser differential refractometer at 25°C and a wavelength of 632.8 nm. The dn/dc was found to be 0.106 ml g^{-1} for a PVC sample synthesized at 50°C. This value is in agreement with data in the literature[18,41,54] and was used for all PVC samples, as dn/dc is independent of molecular weight for high-molecular-weight polymer[55].

G.p.c. measurements

A Waters 150-C g.p.c. with differential refractometer detector was used at 40°C with THF of h.p.l.c. (high-performance liquid chromatography) grade as mobile phase. Five columns (TSK) with the following specifications were used: G1000H8, G2500HXL, G3000HXL, G4000H8 and G7000HXL of exclusion limits 10^3, 2×10^4, 6×10^4, 4×10^5 and 4×10^8, respectively. The flow rate was 1 ml min^{-1}. About 0.1 ml of PVC–THF solutions containing about 0.1 wt% PVC were injected.

G.p.c. calibration

Calibration is an important issue for application of g.p.c.[56,57]. A computer search method for two parameters that are combinations of the Mark–Houwink constants of polystyrene standards and the polymer under study was suggested[58–60]. Mori[58] and Chiantore *et al.*[59] used two broad *MWD* samples and Schroder *et al.*[60], more recently, used more than two samples to calibrate g.p.c. In the present work, the arithmetic method was modified to estimate the calibration parameters with 20 samples measured by LALLS.

Using universal calibration[53], one may write the molecular-weight relationship between PVC and polystyrene (PS) standards as:

$$(M_{PVC})_i = A(M_{PS})_i^B \tag{62}$$

where

$$A = \left(\frac{K_{PS}}{K_{PVC}}\right)^{(1/1+a_{PVC})} \qquad B = \frac{1+a_{PS}}{1+a_{PVC}}$$

Hence, weight-average molecular weight of PVC sample i can be expressed as:

$$\bar{M}_{w,i} = A \int_0^\infty F_i(t) M_{PS}(t)^B \, dt \tag{63}$$

Here $F_i(t)$ is the normalized g.p.c. response at retention time t, and $M_{PS}(t)$ is the molecular weight of PS at retention time t, which can be expressed as a third-degree polynomial with regard to retention time.

If n weight-average molecular weights of PVC are given, then the parameters A and B can be found using a non-linear regression method based on the following equations:

$$\sum_{i=1}^{n-1} \left(\frac{\bar{M}_{w,i+1}}{\bar{M}_{w,i}} - \frac{\int_0^\infty F_{i+1}(t) M_{PS}(t)^B \, dt}{\int_0^\infty F_i(t) M_{PS}(t)^B \, dt} \right)^2 = \min \tag{64}$$

$$\sum_{i=1}^{n} \left(\bar{M}_{w,i} - A \int_0^\infty F_i(t) M_{PS}(t)^B \, dt \right)^2 = \min \tag{65}$$

where $\bar{M}_{w,i}$ are measured by LALLS and $F_i(t)$ and $M_{PS}(t)$ are measured by g.p.c.

Given A and B, the molecular-weight averages and *MWD* can be calculated by routine procedures using g.p.c. detector responses. This method does not require prior knowledge of the specific Mark–Houwink constants for both PS standards and PVC samples. In other words, errors in Mark–Houwink constants of PS standards and PVC will not affect the molecular-weight calculation as long as A and B satisfy equations (64) and (65). In addition, if the universal calibration method is not valid, this method corrects for this potential error.

RESULTS AND DISCUSSION

Comparison of molecular weights measured by different methods

It is well known that PVC molecules can form aggregates in solution and this can cause large errors in molecular-weight measurements even with good solvents[19,20,22–28,35–42,46–49]. These aggregates can be disintegrated into single molecules by either heat[19,27,38,47] or ultrasonic treatment[19,35]. However, for a wide range of molecular weights (23 000–165 000)[43–45,52] or commercial PVC[30,37,50], there is no evidence of aggregate formation. In the present work, LALLS measurements of the highest molecular-weight PVC synthesized at 40°C were unchanged after heating the THF solution at 95°C for 1 h. No anomalous chromatograms were observed for the PVC samples under study. Therefore, aggregation for PVC polymerized above 40°C was considered negligible. This is in agreement with Abdel-Alim *et al.*'s results for PVC made by the bulk process[38].

Using molecular-weight averages measured by LALLS and g.p.c. data, the parameters A and B in equations (64) and (65) were estimated to be 1.74 and 0.931 respectively.

Mark–Houwink correlation for PS standards in THF is given by:

$$[\eta]_{PS} = 1.47 \times 10^{-4} M_{PS}^{0.702} \tag{66}$$

where $M_{PS} = (\bar{M}_w/\bar{M}_n)^{1/2}$.

Equation (66) was obtained from the data given by American Polymer Standards Corporation[61]. According to the definitions of A and B in equation (62) and parameters in equation (66), one can obtain the Mark–Houwink correlation for PVC–THF at 40°C as follows:

$$[\eta]_{PVC} = 5.30 \times 10^{-5} M_{PVC}^{0.828} \tag{67}$$

In the literature, intrinsic viscosity was correlated to either $\bar{M}_w$ or $\bar{M}_n$[21,24,26]. K_{PVC} is in the range $(0.4–10) \times 10^{-4}$ and a_{PVC} in the range 0.7–0.9 for the PVC–THF system at temperatures 20–30°C. Therefore, the present results shown as equation (67) seem reasonable. It should be mentioned that the accuracy of equation (67) depends on the accuracy of the parameters in equation (66) and on the validity of universal calibration.

The weight-average molecular weights measured by g.p.c. using parameters shown above are in excellent agreement with those measured by LALLS as shown in *Figure 1*. If Bohdanecky *et al.*'s Mark–Houwink constants[26] are used in the g.p.c. calibration, the measured molecular weights are 20% lower than those measured by LALLS as shown in *Figure 1*. From equation (62),

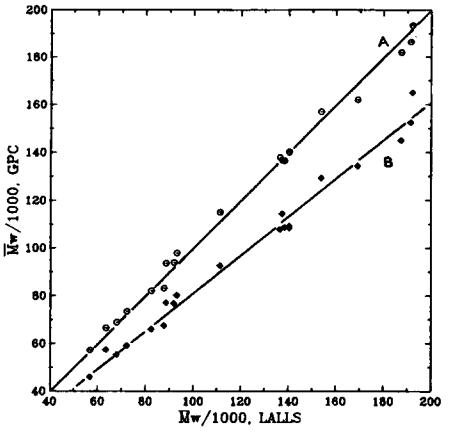

Figure 1 Comparison of weight-average molecular weights measured by different methods. (A, ○) The present method; (B, ◇) $K_{PVC} = 1.5 \times 10^{-4}$, $a_{PVC} = 0.77$ (literature values[26])

one may see that Mark–Houwink correlation with $\bar{M}_w$ or $\bar{M}_n$ may not be suitable for universal calibration. Monodispersed molecular weight or root-mean-square average molecular weights should be used for the universal calibration. This was also demonstrated by Kolinsky *et al.*[29].

Estimation of parameters in the present kinetic model

All of the kinetic parameters estimated in our rate model in a previous publication[16] should be valid in the present model. The remaining parameters will be estimated using molecular-weight information.

According to equations (18) and (32), the parameters τ_i and β_i can be expressed as:

$$\tau_i = \frac{\lambda_i R_{pi}}{(K_p/K_t^{1/2})_i^2 [M]_i^2} + CM_i \qquad (i = 1, 2) \qquad (68)$$

$$\beta_i = \frac{(1-\lambda_i) R_{pi}}{(K_p/K_t^{1/2})_i^2 [M]_i^2} \qquad (i = 1,2) \qquad (69)$$

where

$$K_t = K_{tc} + K_{td} \text{ and}$$

$$\lambda_i = \frac{K_{tdi}}{K_{tdi} + K_{tci}} \qquad (i = 1, 2)$$

the fraction of bimolecular termination by disproportionation, which can be estimated with appropriate molecular-weight information.

The overall rate constant for chain transfer to monomer given in equations (19) and (33) involves five elementary rate constants. K_{fm} should remain constant in both phases, although each phase will have a different value due to the difference in monomer concentrations, at conversions less than X_f. At high conversions ($X > X_f$), however, K_{fm2} is not constant because of the decrease in monomer concentration and the effect of diffusion-controlled reactions. It is necessary to estimate all of the parameters in order to obtain K_{fm2}. In commercial PVC, the concentration of head-to-head structure is very low[17]. Hence, the propagation reaction by head-to-head radical[16] may be negligible so that equation (33) can be simplified to:

$$K_{fm2} = \frac{K_1}{1 + (K_4/K_5)[M]_2} \qquad (70)$$

which was also suggested by Hjertberg *et al.*[13]. Hence, one only has to estimate K_1 and K_4/K_5 to find K_{fm2}.

K_1 and K_4 are head-to-head and head-to-tail propagation rate constants respectively[16]. At high conversions, K_1 may become diffusion-controlled but its sensitivity to environmental effect may not be as great as that for K_{p2}. However, the effect of diffusion control on K_4 can be assumed to be the same as that on K_{p2}. The reaction involving the abstraction of a chlorine atom radical should be chemically controlled over the entire conversion range so that K_5 may be considered constant. Therefore, K_1 and K_4/K_5 can be expressed as a function of free-volume fraction:

$$K_1 = K_{1xf} \exp\left[-CH^*\left(\frac{1}{V_{fp}} - \frac{1}{V_{fxf}}\right)\right] \qquad (X > X_f) \qquad (71)$$

$$K_4/K_5 = (K_4/K_5)_{xf} \exp\left[-B^*\left(\frac{1}{V_{fp}} - \frac{1}{V_{fxf}}\right)\right] \qquad (X > X_f) \qquad (72)$$

where B^* has been estimated in a previous publication[16].

Therefore, the unknown parameters include λ, K_1, K_4/K_5, CH^*, C_p and C_p' for molecular-weight calculations. These parameters were estimated by fitting the present model with weight- and number-average molecular weights simultaneously using a non-linear regression technique. The interesting findings are as follows:

The parameter λ shown in equations (68) and (69) could vary from 0 to 1. It was found that the present model cannot fit the weight- and number-average molecular weights simultaneously if $\lambda > 0$. The best fitting, however, can be achieved by setting $\lambda = 0$ as shown in *Figures 2–6*. This suggests that bimolecular termination of polymer radicals occurs exclusively by combination during VCM polymerization. Razuvayev *et al.*[62] studied the termination mechanism in bulk and suspension polymerization systems using ^{14}C-labelled initiator. They concluded that the average number of end-groups per polymer molecule is between 0.19 and 0.40 but failed to distinguish between combination and disproportionation due to significant chain transfer to monomer. Park *et al.*[63] tried to reduce the importance of chain transfer to monomer using very high initiator levels in solution polymerization and concluded, based on very limited data, that 25% of mutual termination occurs by combination. At very high initiator levels, termination with primary radicals may be significant. Hence, Park *et al.*'s results are open to question. In kinetic modelling, this uncertainty exists in the literature. Mickley *et al.*[64] assumed that all of the termination was by combination. Abdel-Alim *et al.*[5] and more recently Kelsall *et al.*[15] assumed that all of the termination was by disproportionation. This study is the first to estimate λ using molecular-weight information.

In the literature, CM is reported as a constant independent of conversion under certain polymerization temperatures. *Figure 2* shows the effect of CM on weight- and number-average molecular weight over the entire conversion range. If CM is a constant over the entire conversion range, $\bar{M}_w$ should increase significantly and $\bar{M}_n$ increase slightly at high conversions as shown by the long-dashed curve B in *Figure 2*. To fit the experimental data CM must increase with conversion for

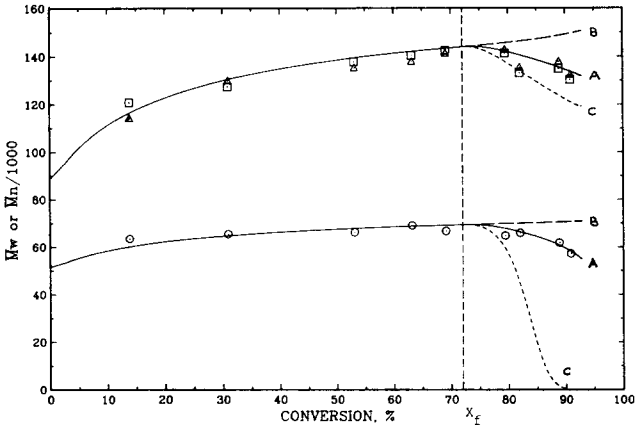

Figure 2 Effect of CM on the accumulated molecular-weight average of PVC at high conversions at 50°C. Perkadox 16-W40 initiator with [I] = 0.15 wt%. (Δ) $\bar{M}_w$ measured by LALLS; (□) $\bar{M}_w$ measured by g.p.c.; (○) $\bar{M}_n$ measured by g.p.c. (A) Model with K_{fm} changing with monomer concentration and free-volume fraction; (B) model with CM as a constant; (C) model with K_{fm} changing with $[M]_2$ only

$X > X_f$. If K_1 and K_4/K_5 were constant and K_{fm2} only affected by $[M]_2$, then CM would increase significantly and, as a result, both $\bar{M}_w$ and $\bar{M}_n$ would decrease dramatically as shown by the short-dashed curve C in *Figure 2*. Therefore, it appears that CM increases slightly at high conversions ($X > X_f$) while K_1 and K_4/K_5 should decrease with conversion. Using equations (70)–(72) to calculate K_{fm2}, the results are shown as a full curve in *Figure 2*, which fits the experimental data well. These measurements further confirm the mechanism of chain transfer to monomer discussed in a previous publication[16]. Decrease in molecular weight at high conversions has been observed experimentally by many other workers[4,11–14]. The effect of monomer concentration on the rate constant of chain transfer to monomer has been discussed by Hjertberg *et al.*[13]. However, this study is the first to estimate K_1 and K_4/K_5 values and to measure the effect of conversion on these parameters.

The fits of the present model with experimental molecular-weight data over the entire conversion range for a wide range of temperature are shown in *Figures 3–6*. One can see that the model fits the experimental data well over the entire range of conversion and temperatures studied. Molecular weight increases slightly with conversion before X_f, then decreases gradually with conversion after X_f. Increase in $\bar{M}_w$ and $\bar{M}_n$ with conversion at $X < X_f$ is due to increase in significance of contribution of the polymer phase. At 60 and 70°C, the model values are slightly lower than experimental data at high conversion stage. Chain transfer to polymer may be more significant at higher temperatures. The parameters estimated from the experimental data shown in *Figures 3–6* are plotted in *Figures 7* and *8*. All the parameters are mild functions of temperature and can be correlated with the following Arrhenius-type equations:

$$K_1 = 5.55 \times 10^{12} \exp(-9340/T) \quad (\text{l mol}^{-1}\,\text{s}^{-1}) \tag{73}$$

$$K_4/K_5 = 4260 \exp(-3410/T) \quad (\text{l mol}^{-1}) \tag{74}$$

$$CH^* = 1.28 \times 10^4 \exp(-3250/T) \tag{75}$$

$$C_p = 8.31 \times 10^9 \exp(-11\,100/T) \tag{76}$$

$$C'_p = 6.48 \times 10^{-3} \exp(-3320/T) \tag{77}$$

With the parameters in equations (73)–(75), one can estimate CM values at any conversion and temperature. Typical values at 50°C are shown in *Figure 9*. One can see that CM is a constant for $X < X_f$, but CM in the

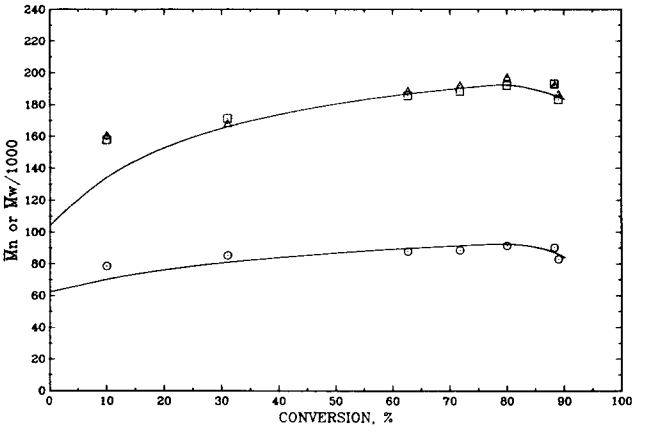

Figure 3 Conversion dependence of accumulated molecular-weight averages at 40°C. Perkadox 16-W40 initiator with [I] = 0.40 wt%. (Δ) $\bar{M}_w$ measured by LALLS; (□) $\bar{M}_w$ measured by g.p.c.; (○) $\bar{M}_n$ measured by g.p.c. (———) Model

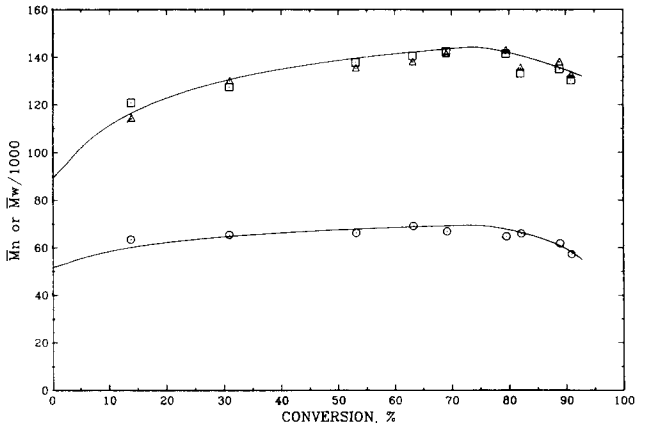

Figure 4 Conversion dependence of accumulated molecular-weight averages at 50°C. Perkadox 16-W40 initiator with [I] = 0.15 wt%. (Δ) $\bar{M}_w$ measured by LALLS; (□) $\bar{M}_w$ measured by g.p.c.; (○) $\bar{M}_n$ measured by g.p.c. (———) Model

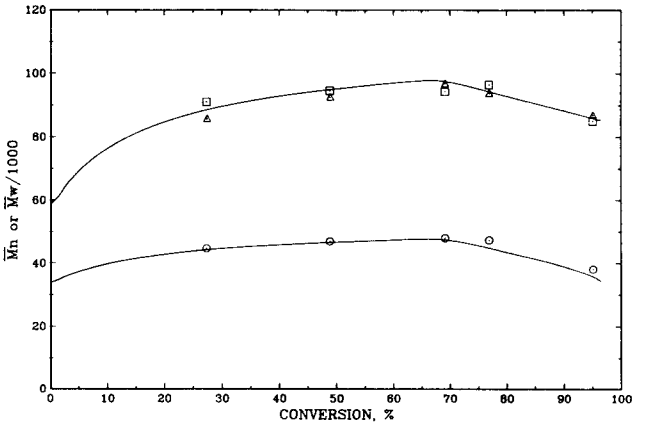

Figure 5 Conversion dependence of accumulated molecular-weight averages at 60°C. Perkadox 16-W40 initiator with [I] = 0.125 wt%. (Δ) $\bar{M}_w$ measured by LALLS; (□) $\bar{M}_w$ measured by g.p.c.; (○) $\bar{M}_n$ measured by g.p.c. (———) Model

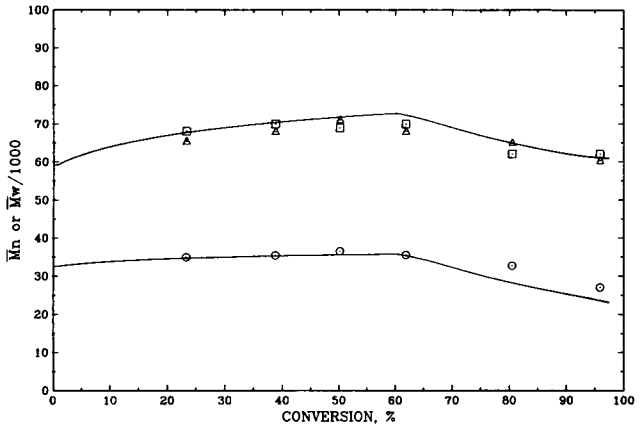

Figure 6 Conversion dependence of accumulated molecular-weight averages at 70°C. Azobisisobutyronitrile (AIBN) initiator with [I] = 0.15 wt%. (Δ) $\bar{M}_w$ measured by LALLS; (□) $\bar{M}_w$ measured by g.p.c.; (○) $\bar{M}_n$ measured by g.p.c. (———) Model

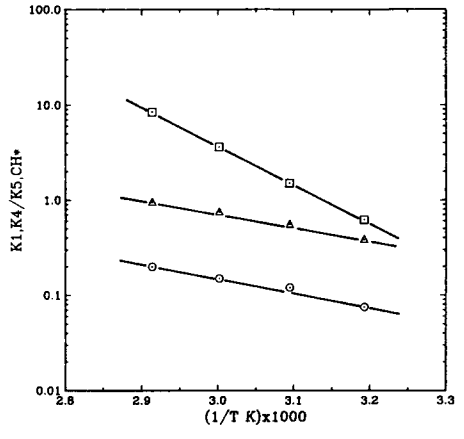

Figure 7 Temperature dependence of kinetic parameters: (○) K_4/K_5, (Δ) CH^*, (□) K_1

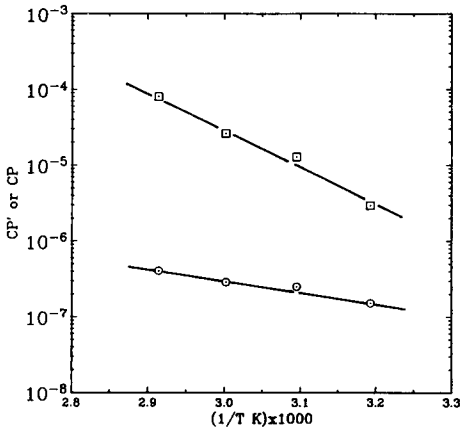

Figure 8 Temperature dependence of C_p and C'_p for VCM polymerization: (○) C'_p, (□) C_p

monomer phase is slightly smaller than that in the polymer phase due to the difference in monomer concentrations in these phases. *CM* in the polymer phase increases significantly after X_f because of the decreasing monomer concentration and the increasing importance of diffusion-controlled reactions. Some typical values of *CM* before X_f are shown in *Table 1*. *CM* values from the literature are summarized in *Table 2*. All the data except Burnett's[70] in *Table 2* are in reasonable agreement at a given temperature. The small differences may be the result of using different models for data interpretation and using samples at different conversions. In fact, the present results are in excellent agreement with the literature data. The *CM* shown in *Figure 9*, for instance, represents all the data at 50°C shown in *Table 2*. *CM* values in *Table 2* estimated from solution polymerization are greater than those in the monomer phase but very close to those in the polymer phase shown in *Table 1*. This is not surprising because the monomer concentrations in solution polymerization are always lower than those for the monomer phase. In solution polymerization, the molecular weight always increases with increase in monomer concentration[64,69,71]. This cannot be explained by the classical mechanism of chain transfer to monomer during VCM

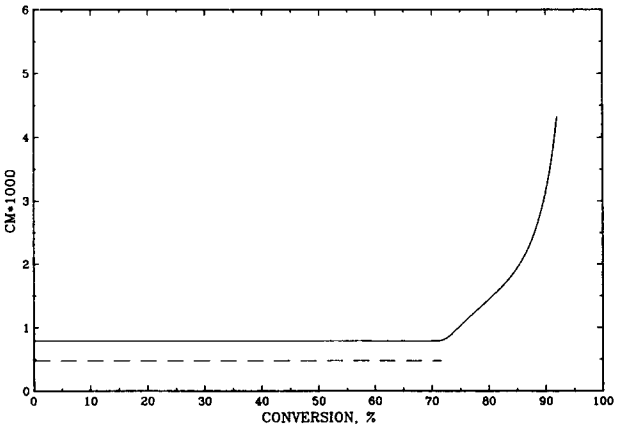

Figure 9 Conversion dependence of *CM* for VCM polymerization at 50°C. (------) *CM* in the monomer phase; (———) *CM* in the polymer phase

Table 1 Some typical values of *CM* for $X < X_f$

Temp. (°C)	$CM \times 10^3$ Monomer phase	$CM \times 10^3$ Polymer phase	Polymerization type
40	0.314	0.508	suspension
50	0.477	0.791	suspension
60	0.723	1.17	suspension
70	1.07	1.58	suspension

Table 2 *CM* values from the literature

Temp. (°C)	$CM \times 10^3$	Polymerization type	Refs.
6	0.171	bulk	4
20	0.32	bulk	65
25	0.385	bulk	4
30	0.63, 0.51, 0.625	bulk	5, 65, 66
40	0.710, 0.71	bulk	4, 65
50	1.10, 1.05, 1.35, 0.85, 1.035	bulk	5, 65–68
60	1.48, 1.23	bulk	65, 67
70	5.71, 2.15, 2.38	bulk	5, 65, 66
25	0.32, 0.0657	solution	69, 70
40	5.0	solution	64
50	1.1, 0.64, 0.78	solution	3, 67
55	0.122	solution	70
60	1.08, 1.28	solution	67
55	1.2 ± 0.2, 1.30	emulsion	12, 13

polymerization. However, according to the present model, K_{fm} will decrease with increasing monomer concentration although other kinetic parameters remain constant under homogeneous conditions; consequently, the molecular weight increases.

C_p and C'_p values for VCM polymerization have never been reported in the literature. C_p is in the range 10^{-4}–10^{-6} and C'_p in the range 10^{-6}–10^{-7} for the temperature range used in this study (see *Figure 8*). These values suggest that chain transfer to polymer is almost insignificant for commercial VCM polymerization. This is in agreement with the results for long-chain branch measurements for commercial PVC[17]. It is also supported by weight- and number-average molecular-weight results[4,5,7,65,72], i.e. weight- and number-average molecular weight increases with conversion slightly at $X < X_f$. If C_p were greater, the weight-average molecular weight would increase significantly particularly at high conversions. Using PVC dimers and trimers as model PVC, Lim *et al.*[73] estimated a C_p of 5×10^{-4} at 50°C, which is one order of magnitude higher than the present value.

Model evaluation

With the parameters estimated above, we are able to evaluate further the present model and explain other features of PVC molecular-weight development. *Figures 10* and *11* show the relationships between instantaneous and accumulated molecular-weight averages. The instantaneous molecular weight in the monomer phase is much lower than that in the polymer phase although *CM* in the polymer phase is higher. The reason is that the termination rate constant is much higher in the monomer phase. The total instantaneous molecular weight is close to that in the polymer phase because the polymer phase dominates the polymerization rate as has been shown previously[16]. The number- and weight-average molecular weights are almost constant at $X < X_f$ due to the low values of C_p and C'_p and other factors are constant. However, the total instantaneous number- and weight-average molecular weights increase gradually due to significant increase in polymerization rate in the polymer phase. The weight-average molecular weight increases slightly because of the effect of chain transfer to polymer. Therefore, the accumulated weight-average molecular weight is slightly lower than the total instantaneous weight-average molecular weight for $X < X_f$. At higher conversions, the instantaneous number- and weight-average molecular weights decrease dramatically due to increase in *CM*. However, the accumulated molecular-weight averages decrease only slightly because of the small amount of polymer produced at this conversion level. These results are in agreement with Hamielec *et al.*'s[74] prediction considering *CM* to be diffusion-controlled and Hjertberg *et al*'s[13] experimental results for polymerization at reduced monomer levels (subsaturation pressure).

The effect of initiator concentration on accumulated molecular-weight averages is shown in *Figure 12*. One can see that the molecular weight decreases slightly with increasing initiator concentration. Again, this result confirms that chain transfer to monomer dominates molecular-weight development. This is consistent with Abdel-Alim *et al.*[5] and Danusso *et al.*'s[65] experimental

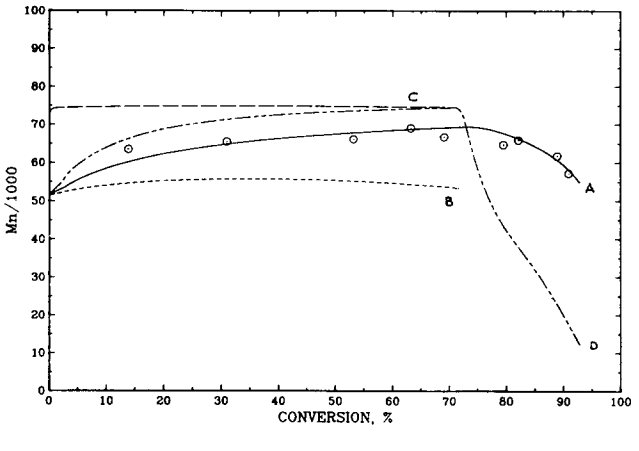

Figure 10 Conversion dependence of instantaneous and accumulated number-average molecular weights at 50°C. Perkadox initiator with [I] = 0.15 wt%. (○) Experimental data. (A) Accumulated number-average molecular weight; (B) instantaneous number-average molecular weight in the monomer phase; (C) instantaneous number-average molecular weight in the polymer phase; (D) the total instantaneous number-average molecular weight

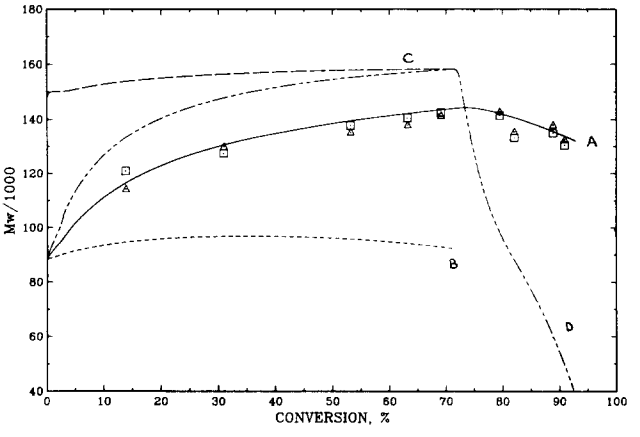

Figure 11 Conversion dependence of instantaneous and accumulated weight-average molecular weights at 50°C. Perkadox 16-W40 initiator with [I] = 0.15 wt%. (Δ) Measured by LALLS; (□) measured by g.p.c. (A) Accumulated weight-average molecular weight; (B) instantaneous weight-average molecular weight in the monomer phase; (C) instantaneous weight-average molecular weight in the polymer phase; (D) the total instantaneous weight-average molecular weight

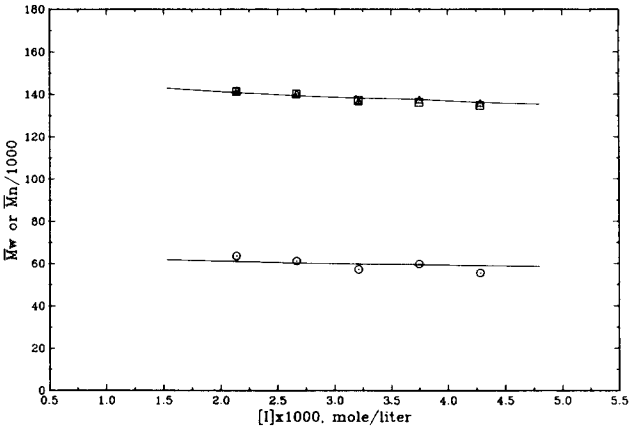

Figure 12 Effect of initiator concentration on accumulated number- and weight-average molecular weights at 50°C. Initiator: Perkadox 16-W40, conversion = 87%. (Δ) $\bar{M}_w$ measured by LALLS; (□) $\bar{M}_w$ measured by g.p.c.; (○) $\bar{M}_n$ measured by g.p.c. (———) Model

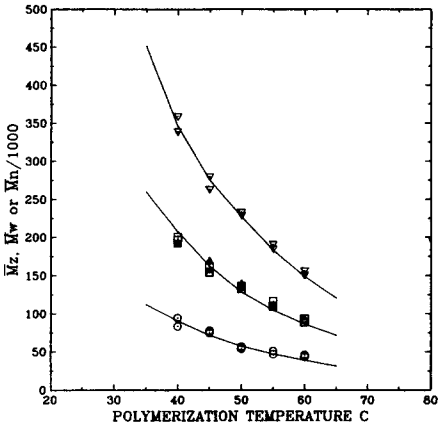

Figure 13 Temperature dependence of accumulated molecular-weight averages. Perkadox 16-W40 initiator with [I] = 0.175%. (▽) $\bar{M}_z$ measured by g.p.c.; (△) $\bar{M}_w$ measured by LALLS; (□) $\bar{M}_w$ measured by g.p.c.; (○) $\bar{M}_n$ measured by g.p.c. (———) Model

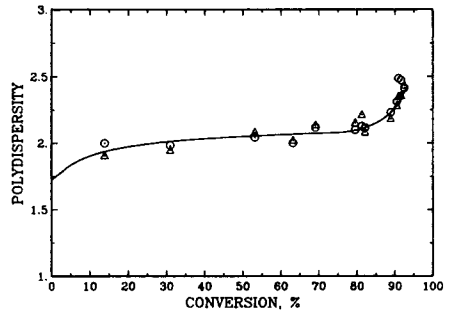

Figure 14 Conversion dependence of polydispersity at 50°C. (○) $\bar{M}_w$ measured by LALLS; (△) $\bar{M}_w$ measured by g.p.c. (———) Model

results. The present model predictions are in excellent agreement with the experimental data.

Figure 13 shows the temperature dependence of $\bar{M}_n$, $\bar{M}_w$ and $\bar{M}_z$ at high conversions ($\simeq$85%). The molecular weight is very sensitive to polymerization temperature as expected. This study provides for the first time experimental measurements and predictions of $\bar{M}_n$, $\bar{M}_w$ and $\bar{M}_z$ as a function of temperature and other reaction variables. The model predictions are in satisfactory agreement with the experimental data over a wide range in temperature (see *Figure 13*).

Given $\bar{M}_w$ and $\bar{M}_n$, one can calculate the polydispersity. Most often, the polydispersity of commercial PVC is between 2.0 and 2.5. Russo *et al.*[4] noticed that the polydispersity of PVC increases with conversion at high conversions. However, this phenomenon has never been predicted quantitatively. *Figure 14* shows a comparison between model prediction and experimental data at 50°C. One can see that the polydispersity increases with conversion and varies in the range 1.7 to 2.5 over the entire conversion range at 50°C. The polydispersity increases slightly when $X < X_f$, which can be attributed to chain transfer to polymer in the polymer phase. At $X > X_f$, the polydispersity increases significantly, and this can be explained as due to chain transfer to monomer and polymer under diffusion-controlled reaction conditions. The number-average molecular weight is independent of chain transfer to polymer but very sensitive to chain transfer to monomer and it decreases significantly with increasing CM. On the other hand, the effect of chain transfer to polymer on the weight-average molecular weight becomes more significant with increasing conversion although the C_p is very low; thus, $\bar{M}_w$ decreasing with conversion is not as significant as $\bar{M}_n$. Consequently, the polydispersity increases significantly at high conversions. The present model can satisfactorily describe this phenomenon.

With the parameters estimated above, one can solve equations (26), (49), (50) and (61) for MWD of PVC at any conversion. However, it is not practicable to solve equation (49) r times simultaneously at time t for concentration of polymer with chain length r. The last two terms in equation (50) may be neglected because of low C_p and C'_p values. Thus, the solution of equation (49) is not required for MWD. *Figures 15–18* show the MWD for conversion less than X_f at 40, 50, 60 and 70°C respectively. One can see that the present model prediction is in excellent agreement with the experimental

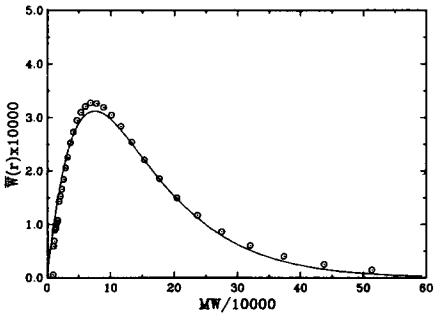

Figure 15 Accumulated molecular-weight distribution at conversion 62.7% ($MW = 62.5r$), temperature 40°C, Perkadox 16-W40 initiator with [I] = 0.40 wt%, $\bar{M}_n = 91.8 \times 10^3$, $\bar{M}_w = 186.6 \times 10^3$. (○) Experimental data. (———) Model

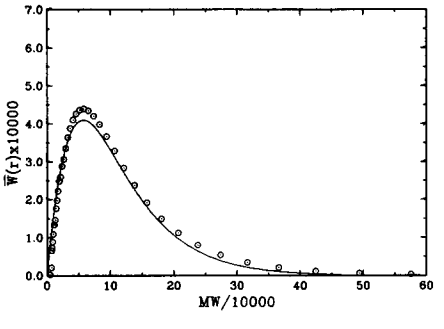

Figure 16 Accumulated molecular-weight distribution at conversion 63.2% ($MW = 62.5r$), temperature 50°C, Perkadox 16-W40 initiator with [I] = 0.15 wt%, $\bar{M}_n = 69.1 \times 10^3$, $\bar{M}_w = 135.2 \times 10^3$. (○) Experimental data. (———) Model

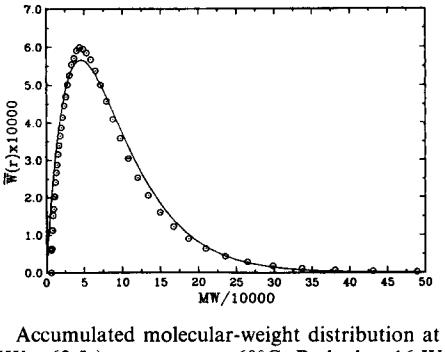

Figure 17 Accumulated molecular-weight distribution at conversion 48.9% ($MW = 62.5r$), temperature 60°C, Perkadox 16-W40 initiator with [I] = 0.125 wt%, $\bar{M}_n = 54.0 \times 10^3$, $\bar{M}_w = 91.1 \times 10^3$. (○) Experimental data. (———) Model

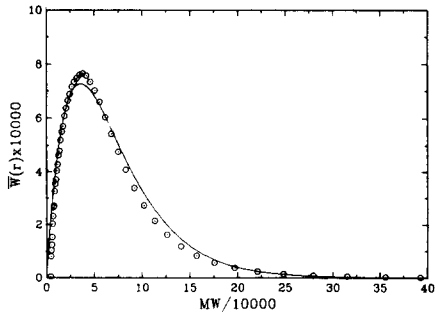

Figure 18 Accumulated molecular-weight distribution at conversion 38.9% ($MW = 62.5r$), temperature 70°C, AIBN initiator with [I] = 0.15 wt%, $\bar{M}_n = 40.4 \times 10^3$, $\bar{M}_w = 66.9 \times 10^3$. (○) Experimental data. (———) Model

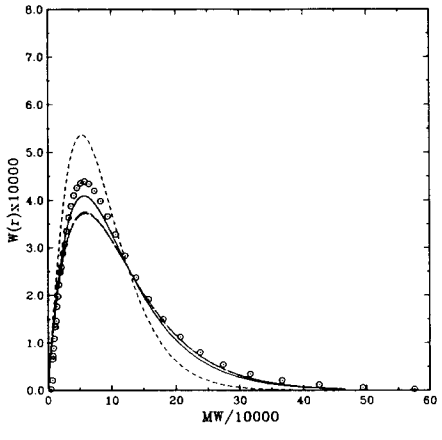

Figure 19 Instantaneous and accumulated molecular-weight distribution at conversion 63.2% ($MW = 62.5r$), temperature 50°C. (○) Experimental data. (———) Accumulated *MWD*; (– – – – –) Instantaneous *MWD* in the monomer phase; (———) instantaneous *MWD* in the polymer phase; (—·—··—) the total instantaneous *MWD*. (Curves – – and —·— overlap)

data. All the distribution curves have similar shape although the distribution shifts to lower molecular weight with increasing polymerization temperature. *Figure 19* further illustrates the contribution of each phase to the accumulated *MWD*. The instantaneous distribution in the monomer phase is narrower than that in the polymer phase. This can be attributed to no chain transfer to polymer and higher termination rate in the monomer phase. However, the contribution of monomer phase to the total *MWD* is very small because polymer is mainly produced in the polymer phase at conversions as high as 63.2%. In fact, the total instantaneous *MWD* is very close to the instantaneous *MWD* in the polymer phase. The total instantaneous *MWD* almost overlaps the accumulated *MWD* for $X < X_f$. However, the instantaneous *MWD* is quite different from the accumulated *MWD* for $X > X_f$ as shown in *Figures 20–23*. One can see that the instantaneous *MWD* shifts to lower molecular weight because of increasing *CM* at high conversion. The amount of this polymer produced at this stage is relatively small. However, this low-molecular-weight PVC may affect the quality of PVC product significantly. For example, the thermal stability of the low-molecular-weight polymer may be much lower. This subject will, however, be discussed in a future publication.

Little work has been done on *MWD* of PVC in the literature[5,40]. This study is the first to describe the *MWD* of PVC both theoretically and experimentally.

From *Figures 10–23*, one can see that the parameters

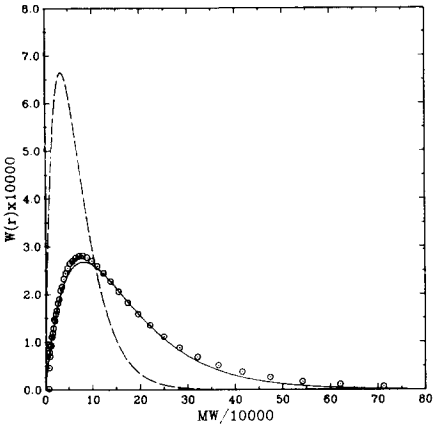

Figure 20 Instantaneous and accumulated molecular-weight distribution at conversion 88.3% ($MW = 62.5r$), temperature 40°C, Perkadox 16-W40 initiator with [I] = 0.175 wt%, $\bar{M}_n = 90.4 \times 10^3$, $\bar{M}_w = 192.8 \times 10^3$. (○) Experimental data. (———) Accumulated *MWD*; (— — —) instantaneous *MWD*

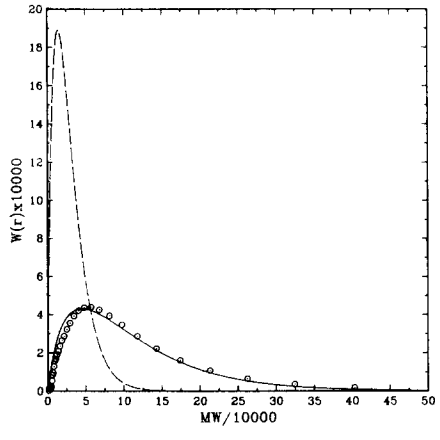

Figure 21 Instantaneous and accumulated molecular-weight distribution at conversion 90.0% ($MW = 62.5r$), temperature 50°C, Perkadox 16-W40 initiator with [I] = 0.15 wt%, $\bar{M}_n = 57.2 \times 10^3$, $\bar{M}_w = 136.9 \times 10^3$. (○) Experimental data. (———) Accumulated *MWD*; (— — —) instantaneous *MWD*

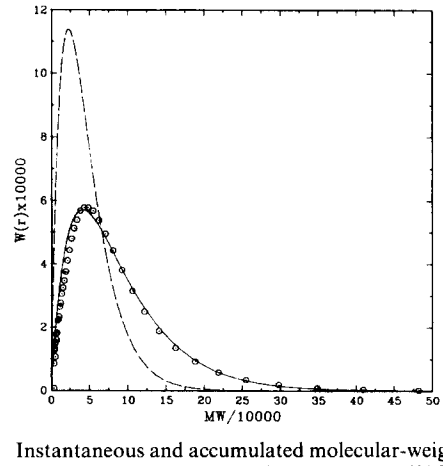

Figure 22 Instantaneous and accumulated molecular-weight distribution at conversion 76.9% ($MW = 62.5r$), temperature 60°C, Perkadox 16-W40 initiator with [I] = 0.125 wt%, $\bar{M}_n = 50.4 \times 10^3$, $\bar{M}_w = 95.6 \times 10^3$. (○) Experimental data. (———) Accumulated *MWD*; (— · · · -) instantaneous *MWD*

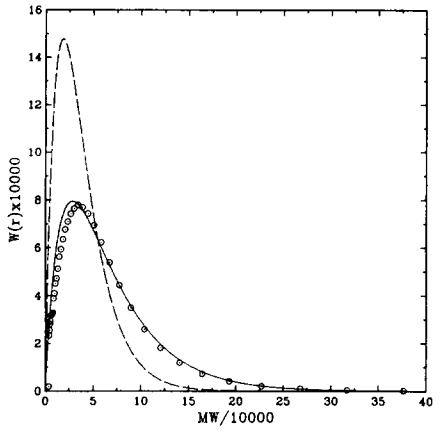

Figure 23 Instantaneous and accumulated molecular-weight distribution at conversion 80.5% ($MW = 62.5r$), temperature 70°C, AIBN initiator with [I] = 0.15 wt%, $\bar{M}_n = 34.7 \times 10^3$, $\bar{M}_w = 66.2 \times 10^3$. (○) Experimental data. (———) Accumulated *MWD*; (– – –) instantaneous *MWD*

estimated above are reasonable. The present model can satisfactorily predict the molecular-weight development of VCM polymerization over the entire conversion range.

CONCLUSIONS

A comprehensive model for molecular-weight development during VCM polymerization has been developed. The model was evaluated using comprehensive molecular-weight average and distribution measurements by LALLS and g.p.c.

The present model is in excellent agreement with experimental rate and molecular-weight data over the entire conversion range of commercial interest for temperatures 40–70°C. The model can satisfactorily describe the kinetic features of VCM polymerization quantitatively, which include molecular-weight averages and distribution as a function of conversion, initiator concentration and polymerization temperature, and can account for the contribution of each phase to the molecular weight of the final polymer at the end of the reactor batch.

Chain transfer to monomer (which involves several elementary reactions) dominates molecular-weight development. *CM* values differ for the two phases and increase significantly for conversions above X_f.

All the parameters estimated based on the present experimental data are given as a function of temperature, which can be used for PVC reactor simulations.

ACKNOWLEDGEMENTS

Financial support from the National Sciences and Engineering Research Council of Canada and The McMaster Institute for Polymer Production Technology is appreciated.

NOMENCLATURE

a = Mark–Houwink constant
A = a parameter defined in equation (62)
B = a parameter defined in equation (62)
B^* = free-volume factor used in K_4/K_5 equation
C = a parameter defined in equation (49)
CH^* = free-volume factor used in K_1 equation
$[Cl^\cdot]$ = chlorine radical concentration (mol l^{-1})
CM = ratio of K_{fm} to K_p
C_p = ratio of K_{fp} to K_p
C'_p = ratio of K'_{fp} to K'_p
$F(t)$ = normalized g.p.c. response, fraction
K = Mark–Houwink constant
K_{de} = radical desorption rate constant (s^{-1})
K_{fm} = chain transfer to monomer rate constant ($l\ mol^{-1}\ s^{-1}$)
K_{fp} = chain transfer to polymer rate constant ($l\ mol^{-1}\ s^{-1}$)
K'_{fp} = $Cl^\cdot$ transfer to polymer rate constant ($l\ mol^{-1}\ s^{-1}$)
K_p = propagation rate constant ($l\ mol^{-1}\ s^{-1}$)
K'_p = $Cl^\cdot$ propagation rate constant ($l\ mol^{-1}\ s^{-1}$)
K_{tc} = combination termination rate constant ($l\ mol^{-1}\ s^{-1}$)
K_{td} = disproportionation termination rate constant ($l\ mol^{-1}\ s^{-1}$)
m = instantaneous mass fraction of polymer
[M] = concentration of monomer (mol l^{-1})
M_n = instantaneous number-average molecular weight
$\bar{M}_n$ = accumulated number-average molecular weight
M_w = instantaneous weight-average molecular weight
$\bar{M}_w$ = accumulated weight-average molecular weight
M_z = instantaneous *Z*-average molecular weight
$\bar{M}_z$ = accumulated *Z*-average molecular weight
PQ_2 = a parameter defined in equation (43)
PQ_3 = a parameter defined in equation (43)
P_r = mole number of dead polymer with chain length r
$[P_r]$ = concentration of dead polymer with chain length r (mol l^{-1})
Q_i = the ith moment of dead polymer distribution
r = polymer chain length
r_c = the critical chain length to precipitate
$[R^\cdot]$ = the total concentration of radicals (mol l^{-1})
R_{cm} = a parameter defined in equations (17) and (18)
R_I = initiation rate (mol $l^{-1}\ s^{-1}$)
R_p = dX/dt, conversion fraction per unit time
R_{pi} = polymerization rate in the i phase (mol $l^{-1}\ s^{-1}$)
RQ_2 = a parameter defined in equation (46)
RQ_3 = a parameter defined in equation (46)
$R_r^\cdot$ = mole number of polymer radical with chain length r
$[R_r^\cdot]$ = concentration of radical with chain length r (mol l^{-1})
S_1 = a parameter defined in equation (22)
S_2 = a parameter defined in equation (43)
t = time
T = absolute temperature (K)
V = volume of reaction system (l)
V_{fp} = free-volume fraction of polymer
V_{fxf} = free-volume fraction of polymer at X_f
$W(r)$ = instantaneous weight fraction of dead polymer with chain length r
$\bar{W}(r)$ = accumulated weight fraction of dead polymer with chain length r
X = conversion, fraction
X_f = critical conversion at which the monomer phase is consumed
Y_i = the ith moment of polymer radical distribution

Greek letters

β_i = a parameter defined in equations (17), (18) and (69)

$[\eta]$ = intrinsic viscosity (dl g^{-1})
λ_i = a parameter defined in equations (68) and (69)
τ_i = a parameter defined in equations (17), (18) and (68)
$\bar{\Psi}$ = a function defined in equation (60)

Subscripts

1 = monomer phase
2 = polymer phase
m = monomer phase
p = polymer phase

REFERENCES

1 Bengough, W. I. and Noirrish, R. D. W. *Proc. R. Soc.* (*A*) 1950, **200**, 301
2 Pezzin, G., Talamini, G. and Vidotto, G. *Makromol. Chem.* 1961, **43**, 12
3 Vidotto, G., Crosato-Arnaldi, A. and Talamini, G. *Makromol. Chem.* 1968, **114**, 217
4 Russo, S. and Stannett, V. *Makromol. Chem.* 1971, **143**, 57
5 Abdel-Alim, A. H. and Hamielec, A. E. *J. Appl. Polym. Sci.* 1972, **16**, 783
6 Cebollada, A. F., Schmidt, M. J., Farber, J. N., Capiati, N. J. and Valles, E. M. *J. Appl. Polym. Sci.* 1989, **37**, 145
7 Pan, Z., Zhai, X., Weng, Z. and Huang, Z. 'Polymer Reaction Engineering' (Eds K. H. Reichert and W. Geiseler), VCH Verlag, Weinheim, 1989, p. 302
8 Talamini, G. and Vidotto, G. *Makromol. Chem.* 1961, **50**, 129
9 Talamini, G. and Vidotto, G. *Makromol. Chem.* 1962, **53**, 21
10 Sorvik, E. M. *J. Polym. Sci., Polym. Lett. Edn* 1976, **14**, 735
11 Sorvik, E. M. and Hjertberg, T. *J. Macromol. Sci.–Chem.* (*A*) 1977, **11**, 1349
12 Hjertberg, T. and Sorvik, E. M. *J. Polym. Sci., Polym. Chem. Edn* 1978, **16**, 645
13 Hjertberg, T. and Sorvik, E. M. *J. Polym. Sci.* (*A*) *Polym. Chem.* 1986, **24**, 1313
14 Liegeois, J. M. *J. Macromol. Sci.–Chem.* (*A*) 1977, **11**, 1379
15 Kelsall, D. G. and Maitland, G. C. 'Polymer Reaction Engineering' (Eds K. H. Reichert and W. Geiseler), Hanser, Munich, 1983, p. 131
16 Xie, T. Y., Hamielec, A. E., Wood, P. E. and Woods, D. R. *Polymer* in press
17 Hjertberg, T. and Sorvik, E. M. 'Degradation and Stabilisation of PVC' (Ed. E. D. Owen), Elsevier Applied Science, London, 1984, p. 21; *Polymer* 1983, **24**, 673
18 Laker, D. *J. Polym. Sci.* 1957, **25**, 122
19 Hengstenberg, J., Schuch, E. and Stuart, H. A. *Makromol. Chem.* 1964, **74**, 55
20 Freeman, M. and Manning, P. P. *J. Polym. Sci.* (*A*) 1964, **2**, 2017
21 McKinney, P. V. *J. Appl. Polym. Sci.* 1965, **9**, 583
22 Vavra, J., Lapcik, J. and Sabados, J. *J. Polym. Sci.* (*A-2*) 1967, **5**, 1305
23 Pezzin, G. and Gligo, N. *J. Appl. Polym. Sci.* 1966, **10**, 1
24 Pezzin, G., Sanmartin, G. and Zilio-Grandi, F. *J. Appl. Polym. Sci.* 1967, **11**, 1539
25 Kolinsky, M., Ryska, M., Bohdanecky, M., Kratochvil, P., Solc, K. and Lim, D. *J. Polym. Sci.* (*C*) 1967, **16**, 485
26 Bohdanecky, M., Solc, K., Kratochvil, P., Kolnsky, M., Ryska, M. and Lim, D. *J. Polym. Sci.* (*A-2*) 1967, **5**, 343
27 Kratochvil, P., Bohdanecky, M., Solc, K., Kolinsky, M., Ryska, M. and Lim, D. *J. Polym. Sci.* (*C*) 1968, **23**, 9
28 Kratochvil, P., Petrus, V., Munk, P., Bohdanecky, M. and Solc, K. *J. Polym. Sci.* (*C*) 1967, **16**, 1257
29 Kolinsky, M. and Janca, J. *J. Polym. Sci., Polym. Chem. Edn* 1974, **12**, 1181
30 Crugnola, A. and Danusso, F. *Polym. Lett.* 1968, **6**, 535
31 Goedhart, D. and Opschoor, A. *J. Polym. Sci.* (*A-2*) 1970, **8**, 1227
32 de Vries, A. J., Bonnebat, C. and Carrega, M. *Pure Appl. Chem.* 1971, **26**, 209
33 Bengough, W. I. and Grant, G. F. *Eur. Polym. J.* 1971, **7**, 203
34 Chan, R. K. S. *Polym. Eng. Sci.* 1971, **11**, 152
35 Rudin, A. and Benschop-Hendrychovra, I. *J. Appl. Polym. Sci.* 1971, **15**, 2881
36 Vidotto, G., Zannetti, R. and Cavalli, L. *Makromol. Chem.* 1971, **146**, 159
37 Baijal, M. D. and Kauppila, K. M. *Polym. Eng. Sci.* 1971, **11**, 182
38 Abdel-Alim, A. H. and Hamielec, A. E. *J. Appl. Polym. Sci.* 1972, **16**, 1093
39 Abdel-Alim, A. H. and Hamielec, A. E. *J. Appl. Polym. Sci.* 1973, **17**, 3033
40 Lyngaae-Jorgensen, J. *J. Polym. Sci.* (*C*) 1971, **33**, 39
41 Lyngaae-Jorgensen, J. *J. Chromatogr. Sci.* 1971, **9**, 331
42 Lyngaae-Jorgensen, J. H. *Makromol. Chem.* 1973, **167**, 311
43 Maron, S. H. and Lee, M. *J. Macromol. Sci.–Phys.* (*B*) 1973, **7**, 29
44 Maron, S. H. and Lee, M. *J. Macromol. Sci.–Phys.* (*B*) 1973, **7**, 47
45 Maron, S. H. and Lee, M. *J. Macromol. Sci.–Phys.* (*B*) 1973, **7**, 61
46 Daniels, C. A. and Collins, E. A. *J. Macromol. Sci.–Phys.* (*B*) 1974, **10**, 287
47 Andersson, K. B. and Sorvik, E. M. *J. Polym. Sci.* (*C*) 1971, **33**, 247
48 Andersson, K. B., Holmstrom, A. and Sorvik, E. M. *Makromol. Chem.* 1973, **166**, 247
49 Sorvik, E. M. *J. Appl. Polym. Sci.* 1977, **21**, 2769
50 Atkinson, C. M. L. and Dietz, R. *Polymer* 1977, **18**, 408
51 Atkinson, C. M. L., Dietz, R. and Green, J. H. S. *J. Macromol. Sci.–Phys.* (*B*) 1977, **14**, 101
52 Ahmad, N., Ali, S. and Nisar, N. M. *J. Macromol. Sci.–Chem.* (*A*) 1986, **23**, 329
53 Grubisic, Z., Rempp, P. and Benoit, H. *J. Polym. Sci.* (*B*) 1967, **5**, 753
54 Huglin, M. B. 'Light Scattering from Polymer Solutions' (Ed. M. B. Huglin), Academic Press, New York, 1972, p. 280
55 Margerison, D., Bain, D. R. and Kiely, B. *Polymer* 1973, **14**, 133
56 Janca, J. *Adv. Chromatogr.* 1981, **19**, 37
57 Dawkins, J. V. *Chromatogr. Sci. Ser.* **25**, 'Steric Exclusion Liquid Chromatography of Polymers' (Ed. J. Janca), Marcel Dekker, New York, 1984, p. 53
58 Mori, S. *Anal. Chem.* 1981, **53**, 1813
59 Chiantore, O. and Hamielec. A. E. *J. Liq. Chromatogr.* 1984, **7**, 1753
60 Schroder, U. K. O. and Ebert, K. H. *Makromol. Chem.* 1987, **188**, 1415
61 American Polymer Standards Corporation, 'Catalog of Polymer Standards for Research and Development'
62 Razuvayev, G. A., Petukhov, G. G. and Dodonov, V. A. *Polym. Sci. USSR* 1963, **3**, 1020
63 Park, G. S. and Smith, D. G. *Makromol. Chem.* 1970, **131**, 1
64 Mickley, H. S., Michaels, A. S. and Moore, A. L. *J. Polym. Sci.* 1962, **60**, 121
65 Danusso, F. and Sianesi, D. *Chim. Ind.* (*Milan*) 1955, **37**, 695
66 Breitenbach, J. W. *Makromol. Chem.* 1952, **8**, 147
67 Uno, T. and Yoshida, K. *Kobunshi Kagaku* 1958, **15**, 819
68 Danusso, F., Pajar, G. and Sianesi, D. *Chim. Ind.* (*Milan*) 1959, **41**, 1170
69 Ryska, M., Kolinsky, M. and Lim, D. *J. Polym. Sci.* (*C*) 1967, **16**, 621
70 Burnett, G. M. and Wright, W. W. *Proc. R. Soc.* (*A*) 1954, **221**, 41
71 Crosato-Arnaldi, A., Talamini, G. and Vidotto, G. *Makromol. Chem.* 1968, **111**, 123
72 Hlousek, M. and Lanikova, J. *J. Polym. Sci.* (*C*) 1967, **16**, 935
73 Lim, D. and Kolinsky, M. *J. Polym. Sci.* 1961, **53**, 173
74 Hamielec, A. E., Gomez-Valillard, R. and Marten, F. L. *J. Macromol. Sci.–Chem.* (*A*) 1982, **17**, 1005